Chapter 4

NUMERICAL ASSESSMENT OF VARIOUS CONNECTION SYSTEMS

This chapter will be introducing numerical investigations with various types of connection systems. Especially, in order to find out the influence of different sizes of bolt-holes, namely so-called bolt clearance, on the stiffness of connection systems, numerical analysis were performed in this chapter. Four connection systems were introduced which have been used in spatial structures and free-form grid shells, meaning the main characteristics of the systems are comparable to the real one. All types of connection have their own characteristics of various geometrical forms, while considering different bolt clearances, which could be observed on connection systems such as splice and end-face connectors.

For the characteristic of splice connector, system 1, 2 and 3 are introduced here while system 4 reflects the end-face connector´s feature (Figure 4.1). As chapter 3 already showed, all simulation models in this chapter, include such features as material properties, contact modelling of the connected parts with particular consideration of contact surface being given to the bolt modelling. All procedures of FE-analysis could be based on the implementation of FE-analysis in chapter 3, due to the successful accomplishments of numerical analysis performed with the experimental results.

All results of this chapter will be used for the implementation of numerical global buckling tests in the grid shells. The results will be used to figure out the influence of various connection types on the buckling load of global grid shells in chapter 5.

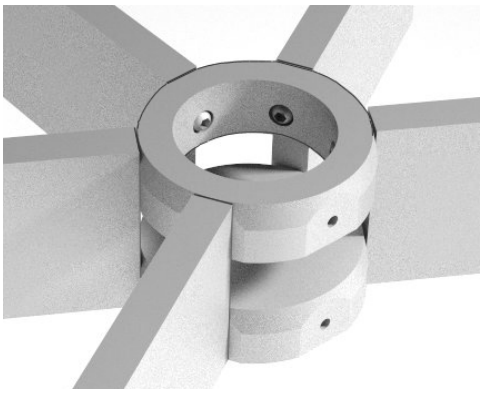

System 1

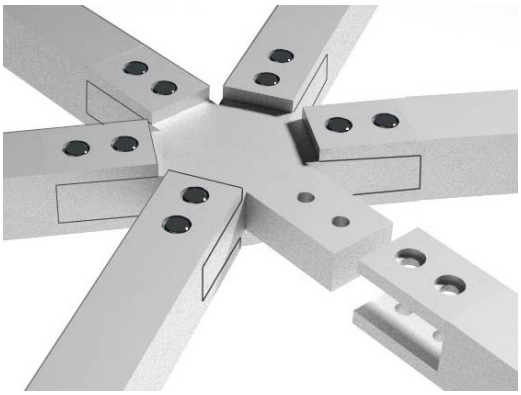

System 2

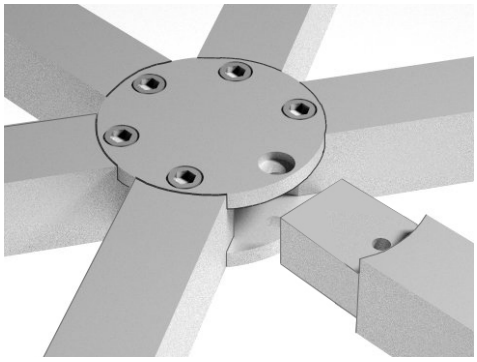

System 3

System 4

Figure 4.1: The four connection systems

4.1 Geometric details of the test

Figure 4.1 presents the models of four node connection systems. System 1 consists of two dish nodes, to which beam members are connected by two screw threads. System 2 is assembled with a solid plate as node with 6 horizontal finger splice plates. The ends of the beam members were fabricated as fork-form fittings, which can be connected to the finger splice plates of the node by two or more counter-sunk bolts in double shear. The third node connection system consists of two flat discs with a circular groove. The beam members are fitted with shear tongues which are then inserted into the grooves of the two discs. The discs and the beam member are connected by bolts.

As for system 4, two flat plates are connected by a single central bolt. Each beam member is connected to the horizontal splice plates by two bolts in single shear plane [Stephan et al 2004].

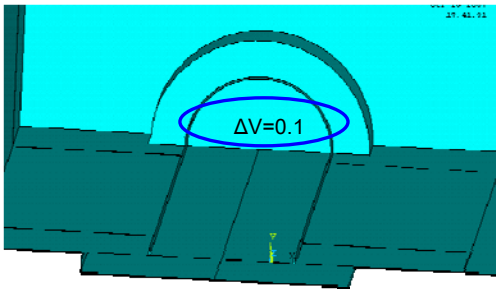

(a)

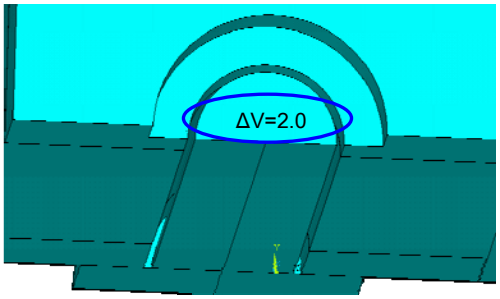

(b)

Figure 4.2:
Deviations of bolt clearances (ΔV=0.1 and 2.0) in the connections (mm)

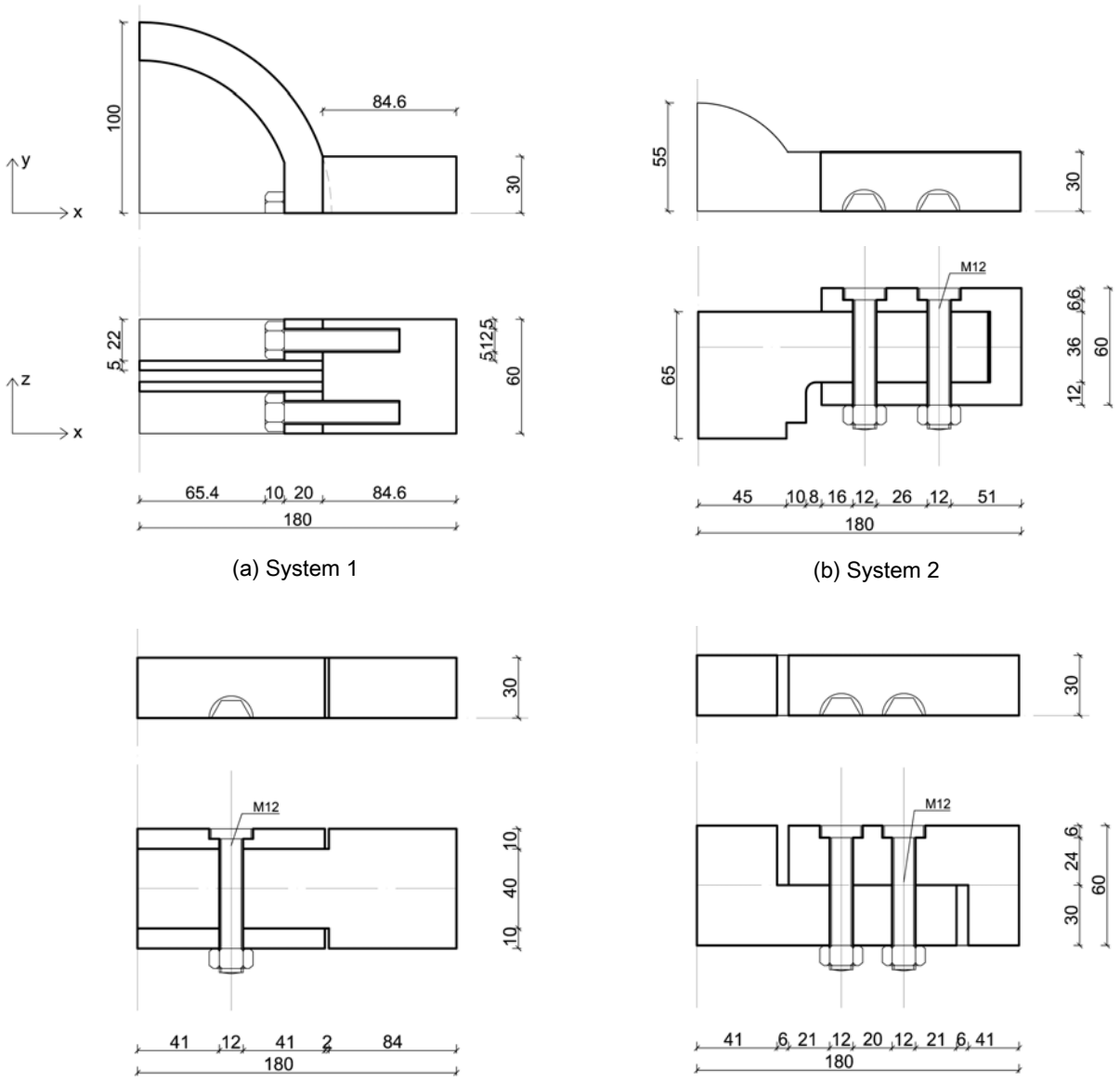

Figure 4.3: Details of four connection systems used in numerical simulations

Two bending tests (My, Mz) and an axial test (F) were performed. Although each model has different geometries, the length (L) of all specimens were assumed to be 180 mm with a cross section b×h=60mm×60mm. Especially, in order to consider the influence of differing sizes of bolt-holes, bolt clearance ΔV=0.1 mm and 2.0 mm were adopted to system 2, 3 and 4 (Figure 4.2). The ΔV of system 1 was assumed as 0 mm, because the bolt connection in system 1 was simulated to be the screw thread type.

4.2 The finite element model

In the finite element model, all elements of the beam, bolts and node were meshed by the 10-node tetrahedral solid structural elements SOLID 92 which was already successfully used in chapter 3. The important interfaces between node and end of beam, as well as the surfaces of bolts, were simulated by creating contact pairs with the 3-D target surface element TARGE 170 and the 3-D 8-node surface-to-surface contact element CONTA 174. To reduce the number of contact planes with saved calculating time, the bolt head or nut and beam element for the bending test around the y-axis (My) are assumed to be fully connected. This simplification may lead to somewhat stiffer deformation, however the overall behavior is not greatly influenced, such as already introduced in other similar literatures [Coelho et al 2006] and from the last chapter, the general deformations of the tests were credible as well. For the bending test around z-axis (Mz) and axial force test (F), the bolt head and beam element could be separated, because of the elongation of bolts. Due to their geometrical symmetry around the central axis, a one-half symmetrical model was used to save computation time.

4.3 Material properties

At first, all the material is assumed to be steel S355, given to a yield strength and elastic modulus of 355 N/mm² and 210000 N/mm², with a Poisson‘s ratio of 0.3, respectively. In order to simplify for plastic behavior, the stress-strain relationship for node and beam was taken as elastically-perfect plastic. Because the high strength bolts included the bolt head and nut, Figure 4.5 shows that the stress-strain curve was applied as a trilinear, with the defining points that have been introduced in other similar literature [Shi et al 2006]. The coefficient of friction (μ) for the contact surface between node and beam was taken as 0.3.

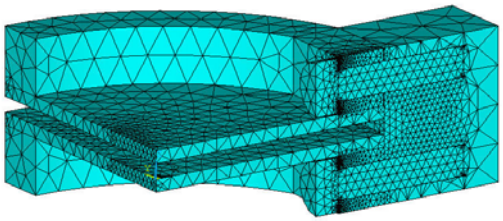

(a) System 1

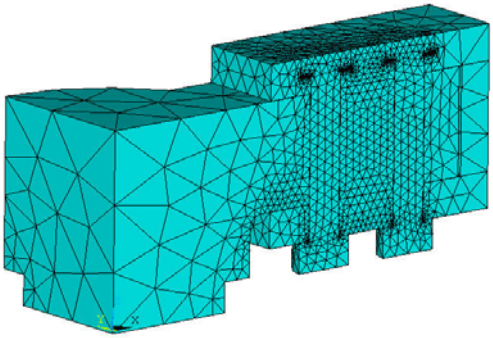

(b) System 2

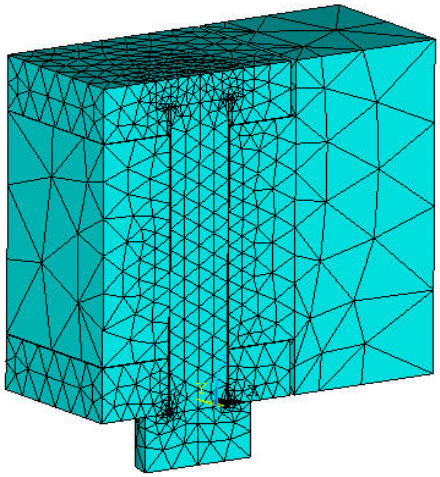

(c) System 3

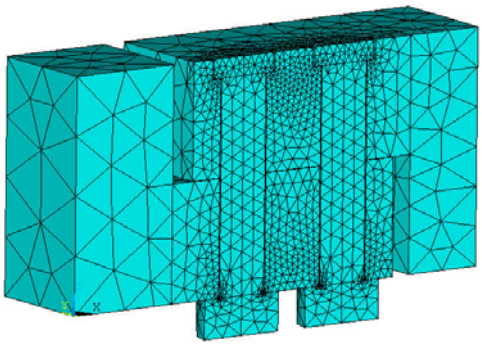

(d) System 4

Figure 4.4: FE-mesh of four models

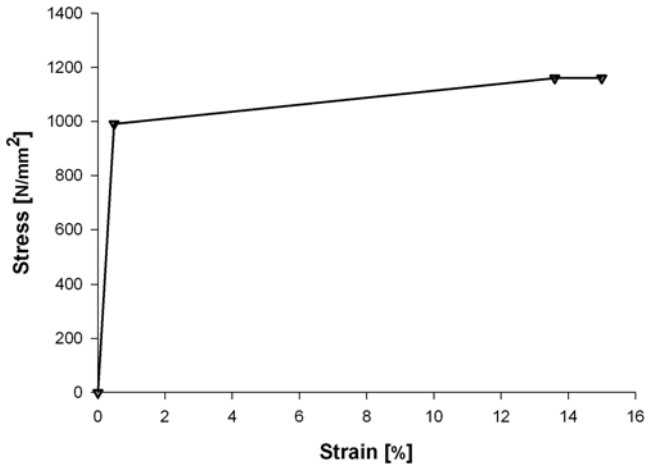

Stress (N/mm²)	Strain (%)
0	0
990	0.483
1160	13.6
1160	15

Figure 4.5: Stress-strain curve for high strength bolts [Shi et al 2006]

4.4 Loading and boundary conditions

The setup for the numerical models is a symmetric cantilever arrangement. In the symmetric plane x-z, the nodes for bending test My and axial test N could be fixed with symmetric geometrical boundary conditions. However, the x-y plane can not meet such a symmetrical condition, since the bolt elongation behavior of Mz is not symmetrical along the x-y plane.

In terms of the load of bending, the end of the node element is fixed and the displacement loading was applied at the end of the beam element. To obtain the axial force, axial displacement loading was applied at the end of the beam. Figure 4.6 shows the definition of moment-rotation relation and load-displacement of axial force tests which have been introduced in other literature related to steel beam-column behavior [Gebbeken et al 1992]. To obtain a more specialized analysis than this typical steel beam-column relationship, a specific analysis tool or formula for each case of connection system may be needed using the same conditions. However, the most significant characteristic of the connection system is the overall behavior of moment-rotation and load-displacement relationships [Coelho et al 2006], so that the influence of connection capacity on the global grid shell can be investigated in the next chapter. This study thusly made use of a simplified definition of bending and axial stiffness.

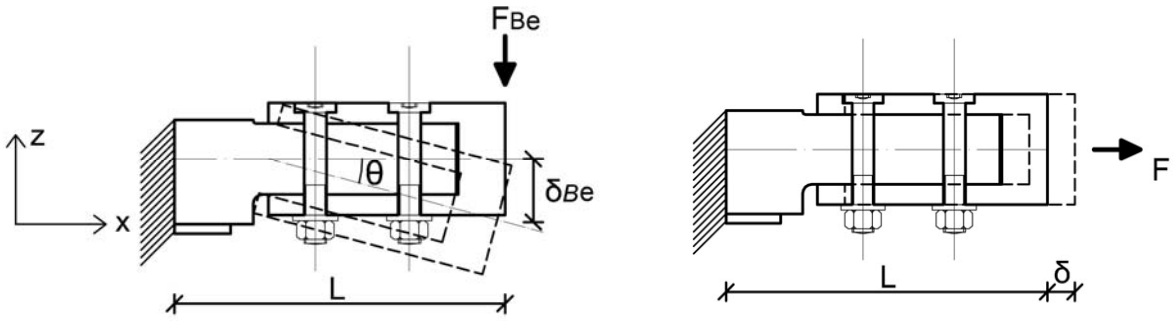

(a) (b)

Figure 4.6: Definition of moment-rotation (a) and axial load-displacement (b) [Gebbeken et al 1992]

The corresponding moment (M) is the product of F_{Be} with the distance L.

$$M = F_{Be} \times L \tag{4.1}$$

The definition of rotation θ is given that the displacement δ_B is divided by the length (L) [Gebbeken et al 1992].

$$\tan\theta = \frac{\delta_{Be}}{L} \approx \theta \quad \text{for} \quad |\theta| < 1 \tag{4.2}$$

4.5 Results of simulations

In the above selected numerical models, bending moment-rotation (My and Mz) and axial-displacement (F) tests were performed. Using two different parameters for bolt clearance 0.1 mm and 2.0 mm, moment-rotation and load-displacement curves of all simulation could be obtained. In each simulation test, the rotation of the joint relative to the node and beam connection is determined from the displaced shapes of connection.

4.5.1 Connection stiffness of axial load (F)

To observe the influence of different bolt clearances easily, system 3 and 4 are introduced in this section. This connection type consists of just one bolt and the geometry of the connector also makes it relatively simple to see the structural behaviors. As introduced for experiment in chapter 3, the pretension was not applied in the bolt .

As show in Figure 4.7, the starting points of the curves are clearly different. The load-displacement curves ΔV=0.1 mm and 2.0 mm start at the displacement 0.05 mm and 0.85 mm, because the whole sizes of bolt clearances were divided by the shank of the bolt. In fact, ΔV=2.0 mm did not start exactly at u=0.1 mm. It should be explained that the stiffness was influenced by strong nonlinear characteristics of contact and target elements which were applied on the shank of the bolt and bolt hole. And the geometry of the beam end is so simple that ΔV could be affected as well. The initial stiffness of ΔV=0.1 mm was higher than the one of 2.0 mm. The reason can be observed by the initial stress distributions (Figure 4.8). From the large deviation between bolt and bolt-hole, such as ΔV=2.0 mm, the load was transferred to the bolt load later than ΔV=0.1 mm. Thus, while the characteristic shear force ($F_{a,R,k}$) of ΔV=0.1 mm reached at the displacement 1.21 mm the load of ΔV=2.0 mm took only around 30% of $F_{a,R,k}$ at this displacement.

However, these two load-displacement curves indicate that ultimate load capacities between two different bolt clearances are almost the same since plastic bearing of the bolt could compensate for the deviation of bolt-holes which

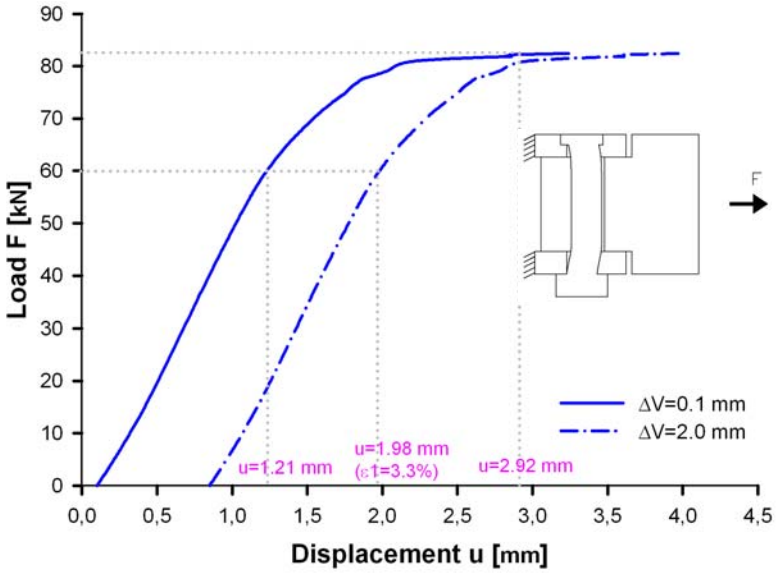

Figure 4.7:
Load-displacement curves of axial load test for connection system 3 with ΔV=0.1 mm and 2.0 mm

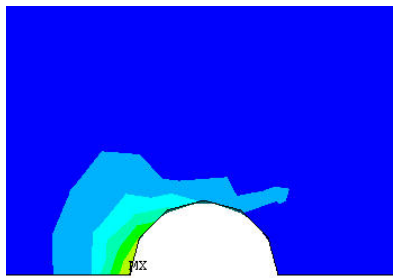

(a) ΔV=0.1 mm

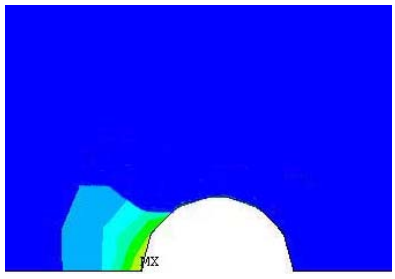

(b) ΔV=2.0 mm

Figure 4.8:
Stress distributions of axial force, connection system 3 at the load level 5 kN

Table 4.1:
Principal strain ε11 in the bolt of axial load test for connection system 3 with ΔV=0.1 mm and 2.0 mm

	$F_{a,R,k}$ = 56.5 kN	F_u = 81.3 kN
ΔV (mm)	ε11 (%)	
0.1	0.90	5.19
2.0	3.30	9.95

leads to similar strength of the bolt. Table 4.1 shows the principal strains (ε11) in the bolt at the characteristic shear force ($F_{a,R,k}$) according to DIN 18800-1 and ultimate shear force (F_u). By means of ε11, the plastic deformation´s capacity is required by the increased ΔV till the characteristic shear force $F_{a,R,k}$. But the actual plastic strain of ultimate shear force F_u is 9.95 % which is clearly smaller than the failure strain of bolt property at 15 % (Figure 4.9). Hence, even though the stiffness of load capacity ΔV=2.0 mm is lower than the value of 0.1 mm, the maximal loading capacity of connection system 3 in bolt clearance 2.0 mm could be maintained as the value of ΔV=0.1 mm.

Due to the geometrical symmetry of the beam, system 2 also has a similar structural behavior of axial load test as system 3. Because the connection system 2 is jointed by two bolts, the general strength of connection is around two times higher than the system 3.

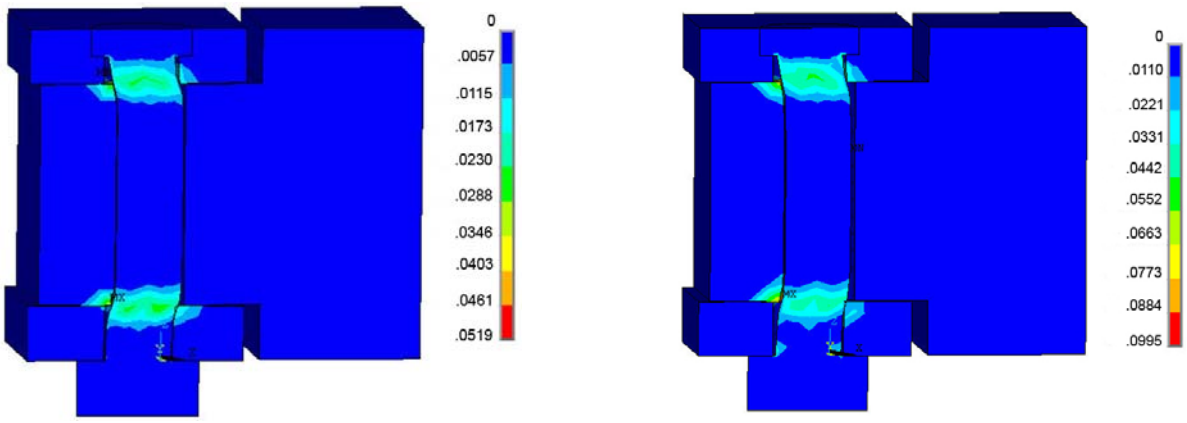

(a) ΔV=0.1 (b) ΔV=2.0 mm

Figure 4.9: Principal strain ε11's distribution of system 3 at ultimate load, (Displacements 5 times enlarged)

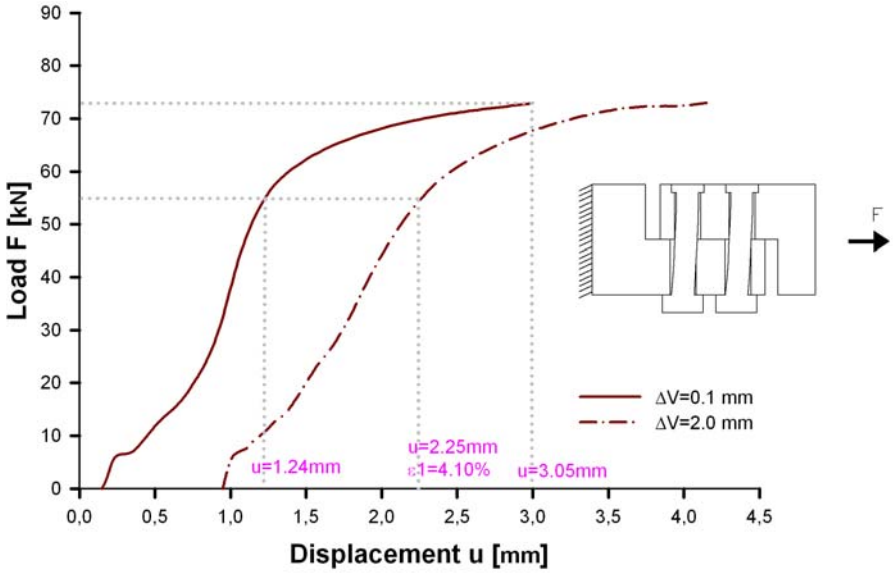

Figure 4.10:
Load-displacement curves of axial load test for connection system 4 with ΔV=0.1 mm and 2.0 mm

On the other hand, system 4 consists of unsymmetrical beam and node due to their L-shaped components which reduce the load bearing capacity. Figure 4.10 shows the load-displacement curves of system 4 in ΔV=0.1 mm and 2.0 mm, respectively. As the curves of system 3, the different stiffness based on various bolt clearances ΔV are shown clearly. That can also be observed by stress distributions in the connections. In Figure 4.11, it is clearly demonstrated that the different processes of stress distributions are caused by bolt clearances. In case of ΔV=0.1 mm, the load of the bolts could be transferred through its small deviations, but the larger ΔV brought the larger displacement of joint. The transfer of bolt load started late due to the large ΔV=2.0 mm, so that the initial stiffness of ΔV=2.0 mm is lower than the case of ΔV=0.1 mm. While the characte-

Table 4.2:
Principal strain ε11 in bolt of axial load test for connection system 4 with ΔV=0.1 mm and 2.0 mm

	$F_{a,R,k}$ = 56.5 kN	F_u = 73 kN
ΔV (mm)	ε11 (%)	
0.1	1.40	4.02
2.0	4.10	8.05

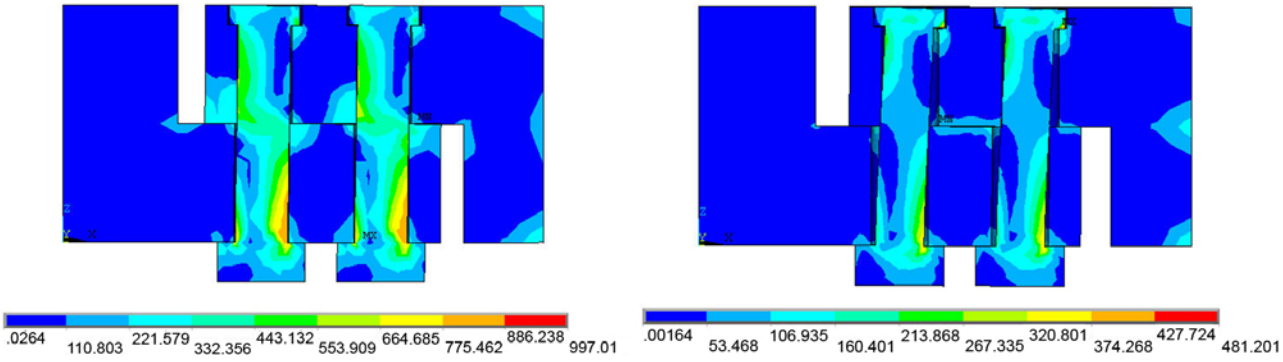

(a) ΔV=0.1 mm (b) ΔV=2.0 mm

Figure 4.11:
Von Mises stress distributions of axial load, connection system 4 at the displacement level 1.24 mm (Displacements 3 times enlarged)

ristic shear load of ΔV=0.1 mm arrived at the displacement 1.24 mm, the load of ΔV=2.0 mm was only 23% of ΔV=0.1 mm.

Figure 4.13 presents all load-displacement curves of axial load tests including four connection systems. Because structural behavior of system 2 is very similar to system 3, again due to the symmetrical geometry of the beam, the detailed explanation is not mentioned, but the general loading capacity of connection is very high and the ultimate load of Δ V=0.1 mm was 158 kN because two parallel bolts in the direction of load could be beared by the shear load effectively.

System 1 shows the highest stiffness among the four systems. As mentioned before, this system is assumed to be fully connected between bolt and beam with a bolt clearance of ΔV=0 mm, which allows the full tension force of the bolts in the joint to be transferred to the beam member by means of the bolt heads (Figure 4.12). Due to without bolt clearance, the initial stiffness of the curve starts at the original displacement level (u=0). And in the sense of geometry between node dishes and beam, there is no discontinuity which leads to a loading transfer well. The maximal load F was over 160 kN which is almost two times higher than system 3.

System 2 and system 4 present very interesting differences influenced by the shapes of connection systems. System 2 has a fork-shaped beam end with two shear planes; tension and compression stresses can be transferred to the beam through two shear planes very effectively. The

stress distribution of system 4, on the other hand, is not effective because the connections are an L-shaped node and beam attached by only one shear plane, so that almost half of the node can transfer bending stress. Thus, for instance, the bending stiffness My of system 4 (ΔV=0.1 mm) is around 50% less than that of system 2.

In relation to bolt clearance ΔV, they show a different mode of behavior. Although the geometrical shape of system 4 caused less stiffness than system 2, the unsymmetrical form with one shear plane was not influenced between ΔV=0.1 and 2.0 mm, because the upper and lower parts of the fork-shaped beam ends of system 2 should move simultaneously with tension and compressive load.

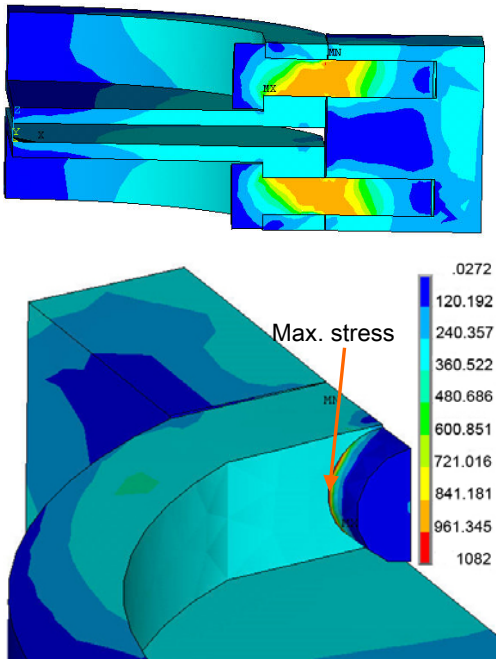

Figure 4.12:
Von Mises stress distributions of axial force, connection system 1

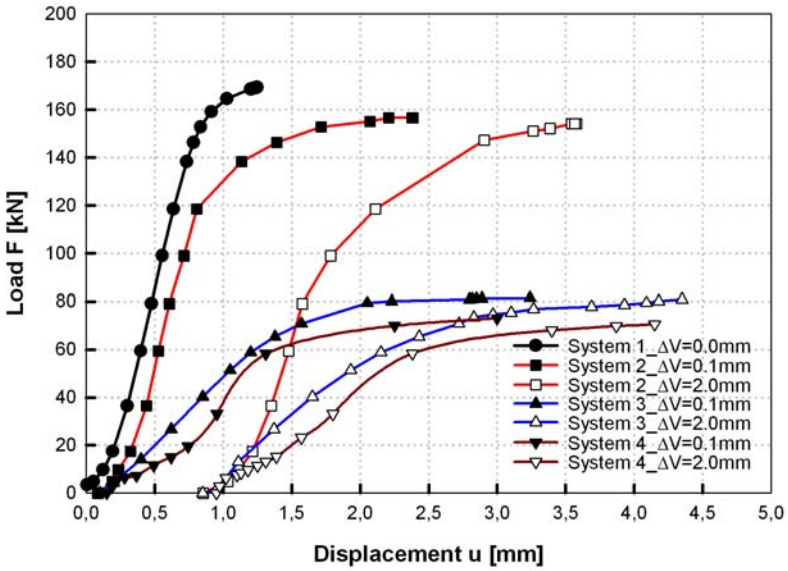

Figure 4.13:
Load-displacement curves of axial load tests for four specimen with ΔV=0.1 mm and 2.0 mm

4.5.2 Connection stiffness of bending moment (My)

At first, the moment-rotation curves (My) of system 2 and 4 are shown in Figure 4.14, because they can explain very clearly the stiffness of connection and the effect of different bolt clearances by their different geometries of connection.

As show in Figure 4.14, the general stiffness of moment-rotation of system 2 is higher than system 4. For example, the rotational elastic capacity of system 2 with Δ V=0.1 mm is about 100 kNm/rad, while system 4 just had 46.8 kNm/rad. The reason can be explained by their structural mechanism of geometrical characteristics. As mentioned before, system 2 consists of a fork-shaped beam member with a splice plate which has two shear surfaces in the connection. Due to the symmetrical behavior of the fork-shaped member, load can be transferred very effectively, and the bolt can bear the shear force well. On the other hand, system 4 just has a single shear surface which was assembled by the L-shaped node and beam member. This causes a nonuniform bending stress which leads to an ineffective transfer of load. This phenomenon can be shown by the stress distribution with reaction force, the evolution of bolt force and

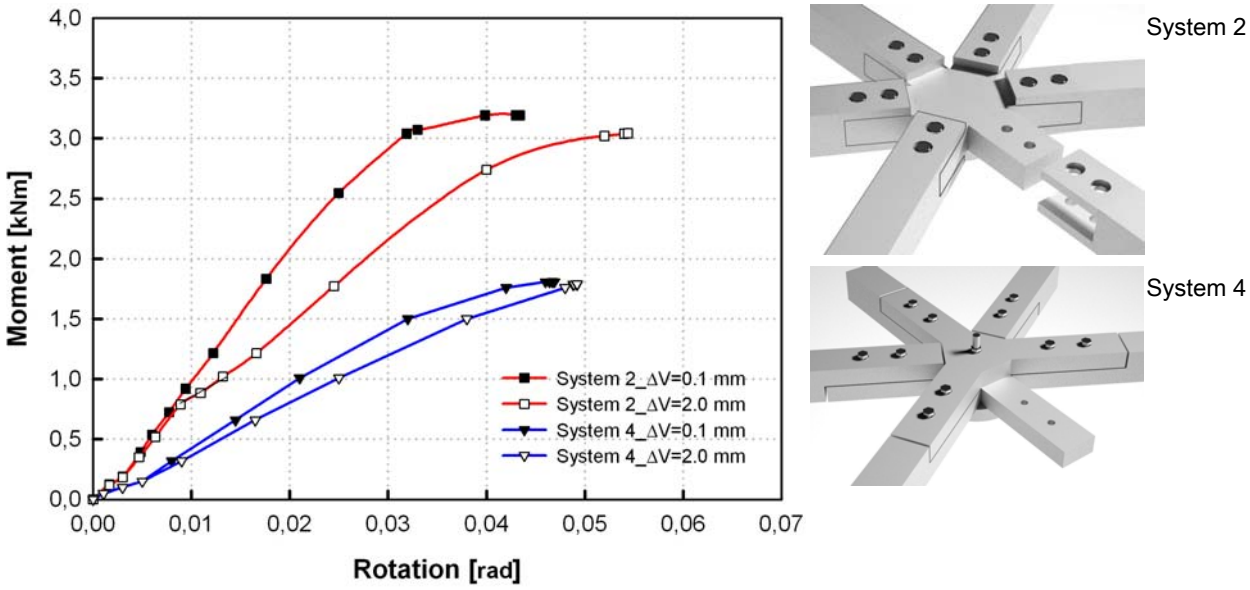

Figure 4.14: Moment-rotation curves (My) of connection system 2 and 4

in the member.

Figure 4.15 shows the stress distribution and reaction contour of system 2. Due to its geometrical characteristics, such as symmetric mechanism based on the fork-shaped beam member, the tensile and compressive loads could be naturally transferred to the end of node, so that general stiffness of the connection is increased. At the same time, this geometry caused a clearly different effect on bolt clearances because the upper and lower parts of the end of member

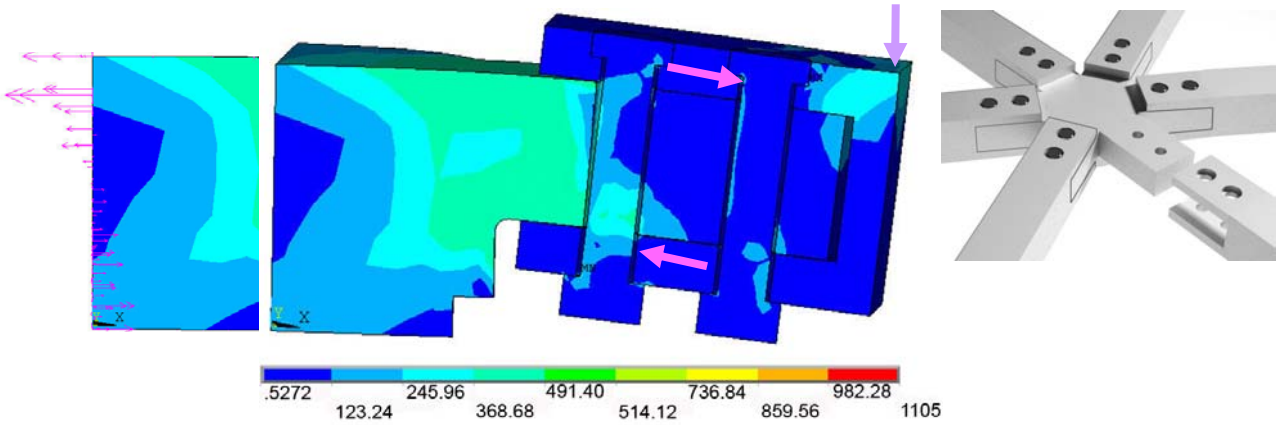

Figure 4.15:
Von Mises stress distribution and reaction of connection system 2 with ΔV=2.0 mm (Displacement 6 times enlarged)

tried to move simultaneously while the vertical load was applied at the end of the beam member.

As for the bolt load, Figure 4.16 shows different behaviors between bolt clearances 0.1 mm and 2.0 mm, while the global bending moment increased in the connection. As the moment-rotation curves in Figure 4.14, bolt loads both of bolt clearances 0.1 mm and 2.0 mm proceeded almost the same until moment level 0.8 kNm where only tension was occurred in the bolt. After that, Figure 4.16 indicates clearly that the lower stiffness of bolt load was transferred to the model of ΔV=2.0 mm because the deviation of bolt and bolt-hole caused a gap until the bolt load could be increased again. From the level of bending moment between 0.8 kNm and 1.0 kNm, the stiffness of bolt loads

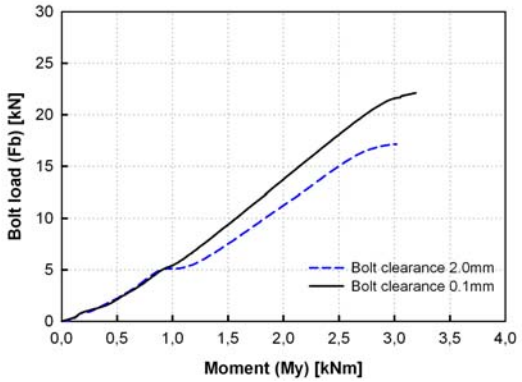

Figure 4.16:
Bolt load and applied bending moment (My) of connection system 2

are different since the bolts are subjected to combined tension and bending which cause the different stiffness of global moment-rotation behaviors based on different bolt clearances. In addition, moment-rotation curve of system 2 with ΔV=2.0 mm shows the maximal bending moment 0.19 kNm lower than the case of ΔV=0.1 mm. It can be explained by the maximal plastic strain of bolt head of ΔV=2.0 mm. Due to the large rotation of the model ΔV=2.0 mm, the maximal plastic strain of bolt head already reached at 14.92 % as a principal strain while the strain of ΔV=0.1 mm was just 10.3 % (Figure 4.17 & Table 4.3).

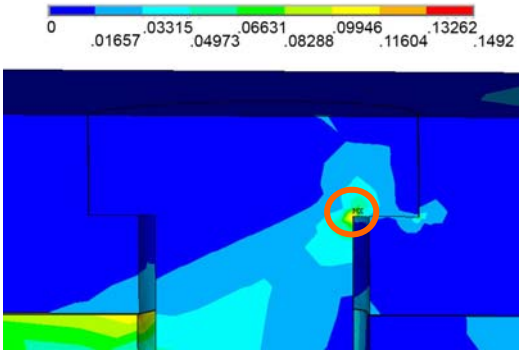

Figure 4.17:
Principal strain of connection system 2 with Δ V=2.0 mm at the bending moment of 3.0 kNm

Table 4.3:
Values of global rotations, ε_{11} and σ_{11} of connection system 2 at the bending moment (My) 3.0 kNm

ΔV (mm)	Rotation (rad)	ε_{11} (%)	σ_{11} (N/mm²)
0.1	0.0425	10.3	940
2.0	0.0525	14.92	1160

Connection system 4, on the other hand, presents a different structural mechanism than connection system 2. Figure 4.18 presents the stress distribution of the connection system 4. Because the node and beam consist of a L-shaped member, they have just one shear surface in the connection. When moment force was applied to the end of the beam member the load transfer was prevented from compressive force to the node and the reaction force in the node was not regular, so that the general bending capacity of this connection system is not sufficient. However, this structural mechanism did not cause a significant deviation of bending stiffness from different bolt clearances.

Figure 4.19 shows the bolt load process with the applied moment in the connection. As shown in this figure, although the case of bolt clearance 0.1 mm

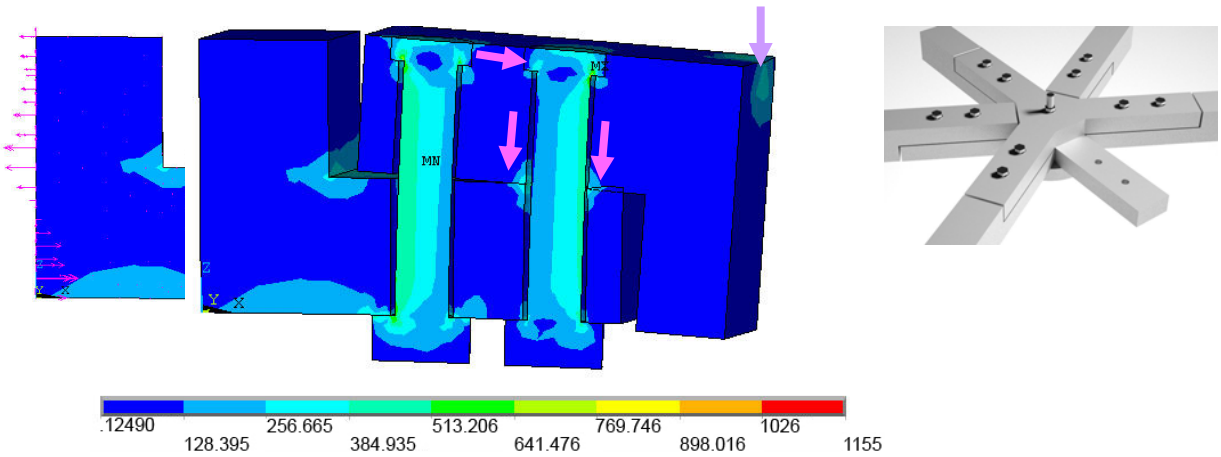

Figure 4.18:
Von Mises stress distribution and reaction of connection system 4 with ΔV=2.0 mm (Displacement 6 times enlarged)

could transfer a little higher force in the bolt, the model of bolt clearance 2.0 mm shows almost the same bolt load process in the connection since the compressive force, which had occurred to the node contact surface by the beam member, was prohibited moving toward the bolt surfaces.

Figure 4.20 presents the moment-rotation curves of all connection systems. Since the connection system 1 was assumed to be fully connected, the curve shows the highest stiffness. The rotational elastic capacity of system 1 is 134.8 kNm/rad and maximal moment capacity is 3.51 kNm. In case of connection

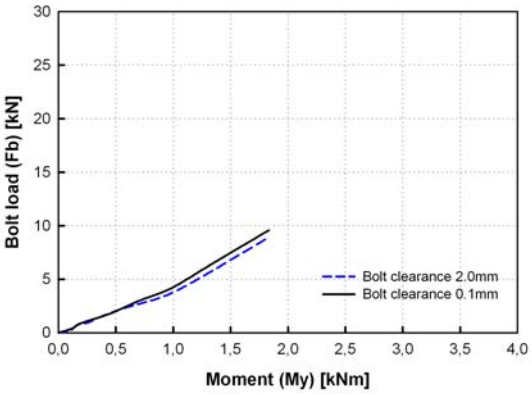

Figure 4.19:
Bolt load and corresponded bending moment (My) of connection system 4

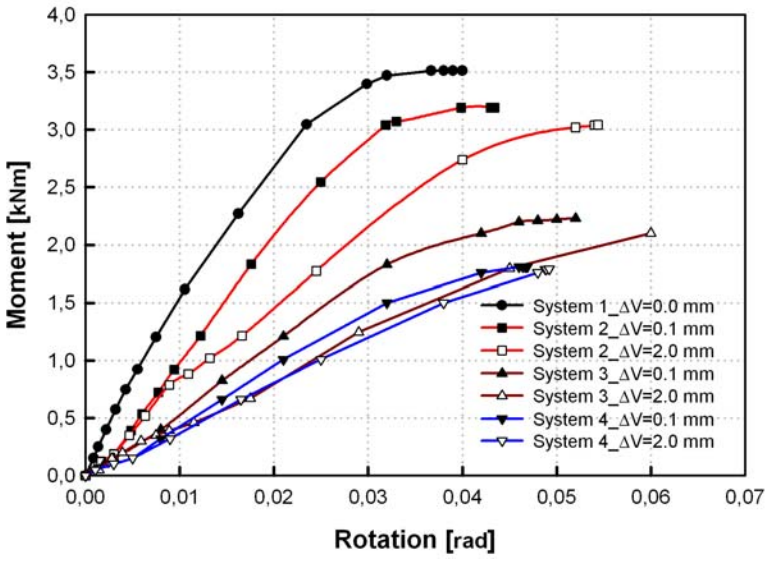

Figure 4.20: Moment-rotation curves (My) of four connection systems

system 3, the structural mechanism is similar with system 2 because this system also consists of two shear planes that a symmetric beam member produces. Also, as in the case of system 2, the different stiffness between bolt clearances 0.1 mm and 2.0 mm is obviously influenced by their geometrical characteristic, which can be observed by the stress distributions of ΔV=0.1 mm and 2.0 mm of system 3, respectively. As shown in Figure 4.21, the small deviation of bolt clearance leads the bolt to be taking the bending load early. Otherwise, the large deviation of bolt clearance 2.0 mm brought a large rotation, so that the bolt could be carried by bending later than the model of ΔV=2.0 mm. In terms of the entire strength of connection, the rotational elastic capacity of the system is 56.3 kNm/rad which is just 50% of system 2 since this system is connected by only one bolt.

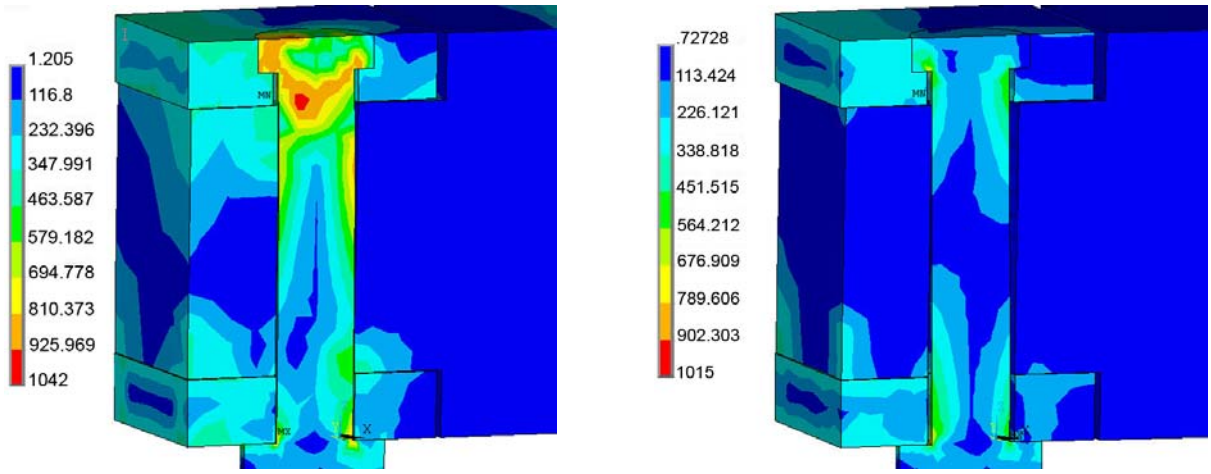

(a) ΔV=0.1 mm (b) ΔV=2.0 mm

Figure 4.21: Von Mises stress distributions of connection system 3 (Displacement 2 times enlarged)

4.5.3 Connection stiffness of bending moment (Mz)

To figure out another nodal stiffness factor, bending moment around z-axis (Mz) of four connection systems were performed. As mentioned in the section 4.4, symmetrical boundary conditions could not be applied since the bolt elongation must be free in the x-y plane. Thus, entire finite elements were modelled in the simulations.

Figure 4.24 shows the moment-rotation curves of all connection systems. As previous axial and bending tests presented, the stiffness and strength of system 1 are the highest, because the connection is assumed to be fully rigidly connected and two bolts bear the bending moment. The rotational elastic capacity of this system is 138.5 kNm/rad which is about 22.2% higher than system 2 with ΔV=0.1 mm. As shown in Figure 4.22, maximal stress was observed in the bolt head.

In case of system 2, it is clearly seen that the entire bending stiffness (Mz) was transferred to two bolts. Figure 4.23 shows the deformation´s figures of two bolts with the distributions of plastic principal strain´s distributions of two bolts. Due to the symmetrical geometry of fork-shaped beam and the positions of bolts, a lever effect, which occurred in the bolts, tried to keep the equilibrium of bending moment.

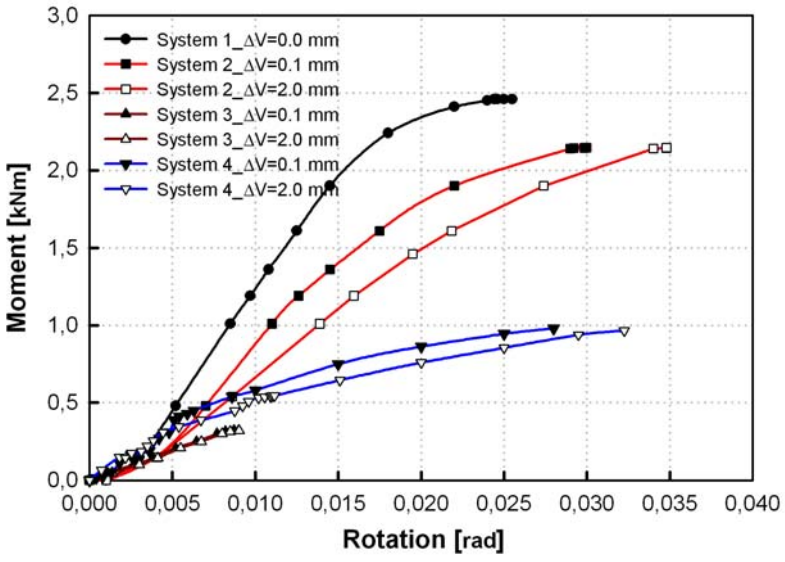

Figure 4.24: Moment-rotation curves (Mz) of four connection systems

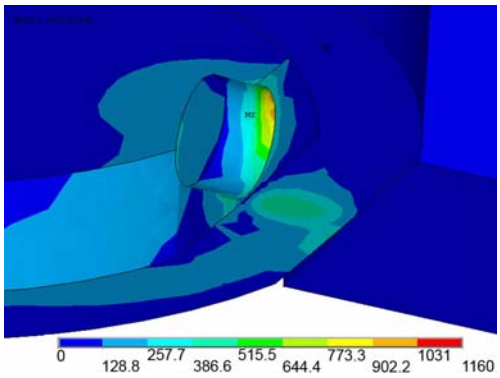

Figure 4.22:
Von Mises stress of connection system 1 (Displacement 2 times enlarged)

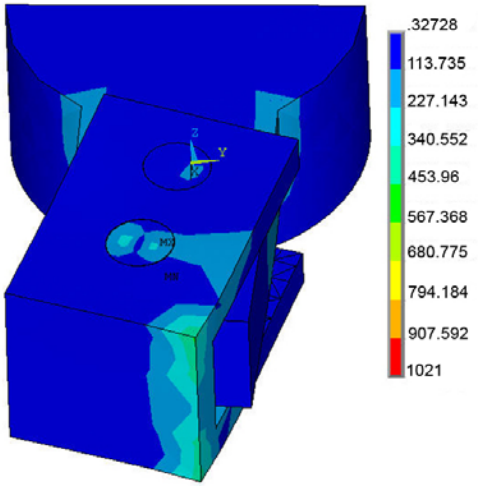

Figure 4.23:
Von Mises stress distribution and deformation of connection system 2 (Displacement 20 times enlarged)

Table 4.4:
Principal strain ε11 in the bolt of bending moment (Mz) for connection system 2 with ΔV=0.1 mm and 2.0 mm

ΔV (mm)	0.1	2.0
ε11 (%)	4.89	9.46

At the same time, even though the different stiffness between ΔV=0.1 mm and 2.0 mm could be observed, the maximal strengths of the bending are almost same. As shown in Table 4.4, the actual plastic strain at the ultimate bending level is 9.46 % which did not reach a failure strain level of 15 %. Therefore, the maximal strength of ΔV=2.0 mm did not fail earlier than the case of ΔV=0.1 mm.

The bending stiffness of system 4 is significantly lower than system 2. For example, the maximal bending moment of this system with ΔV=0.1 mm is more than 50 % lower than system 2. Contrary to system 2, due to its geoemtrical characteristic, the bending moment was transferred to the bolts only through a half of whole beam depth. That caused a severe torsion in the bolt near by the part of nut, which the bolts could not bear a high bending moment (Figure 4.26).

The lowest bending moment could be seen in the connection system 3. The maximal bending moment of ΔV=0.1 mm is just 0.31 kNm. This system is connected by only one bolt, thus the bolt could not play a roll for the lever effect to bear the bending resistance in the connection.

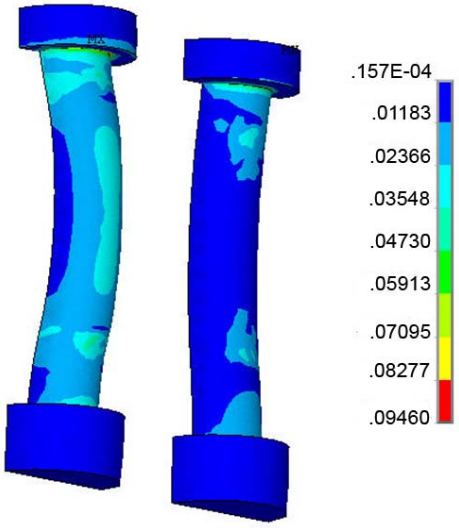

Figure 4.25:
Principal strain ε11 in the bolt of connection system 2 with ΔV=2.0 mm corresponding to Mz (Displacement 20 times enlarged)

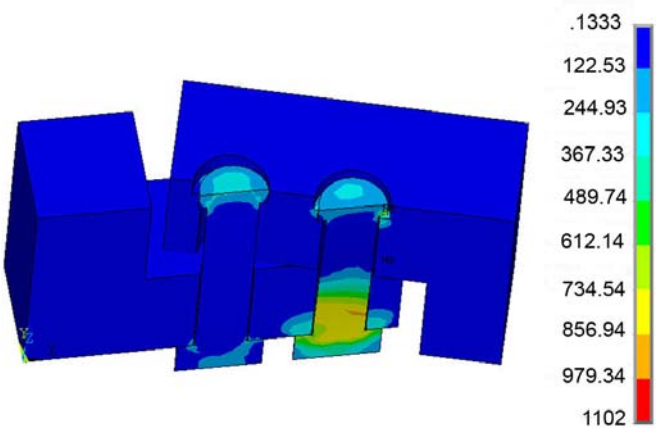

Figure 4.26:
Von Mises stress distribution of connection system 4 with ΔV=0.1mm corresponding to Mz (Displacement 20 times enlarged)

4.6 Summary

Using the finite element method which was already successfully performed in chapter 3 to compare between real experiment and finite element analysis, four connection systems could be simulated to obtain connection´s stiffness, such as axial force-displacement and moment-rotations of My and Mz, respectively. In particular, the different bolt clearances between bolt and bolt-hole of 0.1 mm and 2.0 mm were modeled into the geometry of simulation as parameter factors.

In terms of the numerical analysis for axial force-displacement, system 1 and 2 show very high stiffness. System 1 was assumed to be ΔV=0 mm as a screw thread, thus the tension of two bolts could be fully transferred. Two bolts of system 2 could also bear the shear force effectively due to the geometry of connection. The ultimate load of system 3 was only about 50 % of system 2, even though the failure mechanism is very similar with system 2, because the system is connected only by one bolt. System 4 showed lower stiffness of load displacement curves. Because the L-shaped beam member caused a bending stress in the bolt, the ultimate load of connection was just 73 kN which was 8.3 kN lower than system 3. System 2, 3 and 4 showed very clear different stiffness between ΔV=0.1 mm and 2.0 mm. However, the ultimate loads of ΔV=2.0 mm had identical values of ΔV=0.1 mm because ultimate shear load occurred at a range of the principal plastic strain 8~10 % which did not reach the bolt failure´s property (15 %).

As for the bending moment-rotational capacity around y-axis (My), system 2 and 4 revealed that a large bolt clearance could not always bring a significant lower stiffness than a small ΔV in the connection. Connection system 2, with compressive and tensile forces could be transferred well by symmetrical structural behavior with two shear planes, presented 31.3 % different stiffness of the rotational elastic capacity between ΔV=0.1 mm and 2.0 mm. System 4, however, showed just 4.6 % deviation between ΔV=0.1 mm and 2.0 mm. It can be explained

that L-shaped node and beam member consisted of one shear plane prevented the influence of bolt clearance from bending moment. Maximum bending capacity of system 3 was lower than system 2 because of only one bolt. But this system showed 17.5 % different rotational elastic capacity between ΔV=0.1 mm and 2.0 mm due to its similar structural behaviors as system 2.

Regarding the moment-rotational capacity around z-axis (Mz), general patterns of maximum moment capacities of four connection systems were quiet similar as the result of My. Regardless of different ΔV, however, connection system 3 presented very low bending capacities, because only one bolt could not transfer bending moment in the connection.